View metadata, citation and similar papers at core.ac.uk

brought to you by CORE

provided by Open Archive Toulouse Archive Ouverte

The original publication is available at www3.interscience.wiley.com

http://dx.doi.org/10.1002/jbm.a.30795

Calcium carbonate-calcium phosphate mixed cement compositions for bone reconstruction

C. Combes[1,*], R. Bareille[2], C. Rey[1]

[1]CIRIMAT, UMR CNRS 5085, Equipe Physico-Chimie des Phosphates, ENSIACET, 118 route de Narbonne, 31077 Toulouse cedex 4, France

[2] INSERM U-577, Laboratoire “Biomatériaux et Réparation Tissulaire”, Université Victor Segalen Bordeaux 2,146, rue Léo Saignat, 33076, Bordeaux Cedex, France

Abbreviated title: $CaCO_3$-CaP mixed cement compositions

*Corresponding author. Fax: +33 5 62 88 5773

Email-address: Christele.Combes@ensiacet.fr

Abstract

The feasibility of making calcium carbonate-calcium phosphate ($CaCO_3$-CaP) mixed cements, comprising at least 40 % (w/w) $CaCO_3$ in the dry powder ingredients, has been demonstrated. Several original cement compositions were obtained by mixing metastable crystalline calcium carbonate phases with metastable amorphous or crystalline calcium phosphate powders in aqueous medium. The cements set within at most 1 hour at 37°C in atmosphere saturated with water. The hardened cement is microporous and exhibits weak compressive strength. The setting reaction appeared to be essentially related to the formation of a highly carbonated nanocrystalline apatite phase by reaction of the mestastable CaP phase with part or almost all of the metastable $CaCO_3$ phase. The recrystallization of metastable CaP varieties led to a final cement consisting of a highly carbonated poorly crystalline apatite (PCA) analogous to bone mineral associated with various amounts of vaterite and/or aragonite. The presence of controlled amounts of $CaCO_3$ with a higher solubility than the apatite formed in the well-developed calcium phosphate cements might be of interest to increase resorption rates in biomedical cement and favor its replacement by bone tissue. Cytotoxicity testing revealed excellent cytocompatibility of $CaCO_3$-CaP mixed cement compositions.

Keywords: bone cement, calcium carbonate, calcium phosphate, FTIR spectroscopy, cytotoxicity

New $CaCO_3$-CaP mixed cement compositions

Introduction

Among the large variety of biomaterials now available, an increasing number of calcium phosphate (CaP) ceramics and cements are used as bone substitutes in orthopaedic and maxillo-facial surgery [1]. Fast-setting CaP bone cements have been studied in depth and developed in the last few years essentially as bone filling and bone reinforcement biomaterials due to their excellent biocompatibility and bioactivity. However, even though they can perfectly fill a bone cavity and be shaped as desired [2-10], one of the main concerns of surgeons is to reach higher rates of resorption, an improvement of bone reconstruction and to a lesser extent higher mechanical resistance [11-13].

Several types of setting reaction can be involved in CaP biomimetic cements hardening and many of them lead to the formation of poorly crystalline apatites with a varying degree of crystallization and carbonation. The aim of biomimetic bone cements is to disturb bone functions and properties as little as possible and to behave similarly to bone tissue. From a biological point of vue, this term defines cements which can reproduce the composition, the structure, the morphology and the crystallinity of bone crystals [14].

Bone mineral is described as a poorly crystalline non-stoichiometric apatite and several studies have revealed the existence of non-apatitic, labile environments of mineral ions probably located at the surface of the crystals [15-16]. These specific ion environments have been shown to be directly related to the reactivity of poorly crystalline apatites (PCA) and bone mineral [16-17]. The solubility of apatites depends on the presence of vacancies and the molar Ca/(P+C) ratio (P for phosphate ions and C for carbonate ions) [18]. Carbonate ions can be incorporated into the apatite stucture and substitute for anions (phosphates and/or hydroxide ions) [19]. The lower this ratio, the higher the amount of lacunae and the less the cohesiveness of the crystals which implies higher solubility. Other physical chemical factors such as porosity or the presence of labile non-apatitic environments have been found to affect cement biodegradation properties.

The resorption properties of mineral biomaterials are generally believed to be related to the solubility of their constitutive CaP phases. Several ceramic and cement compositions have been studied to improve the bioactivity and biodegradation properties [14, 20]. For example, the concept of biphasic calcium phosphate (BCP) ceramics is based on the optimum balance between more stable (hydroxyapatite, HA) and more soluble (tricalcium phosphate, TCP) phases to control material resorption [21]. This is based on the dissolution/transformation processes of TCP and HA which depend on several factors such as the composition of the

phases and the sintering temperature and conditions. Another example is coralline HA, a carbonated hydroxyapatite which is prepared by the hydrothermal conversion of calcium carbonate from coral in the presence of ammonium phosphate [22-23]. It has been suggested that controlling the thickness of hydroxyapatite on a $CaCO_3$ matrix could control the rate of resorption of the implant and its replacement by newly formed bone [24]. The concept of biphasic ceramics has however sparsely been developed in view of controlling the resorption of ionic cements [25-29]. Calcium carbonate compounds have a higher solubility than apatite [30-31] and although some mineral cements containing calcium carbonate have already been proposed, the use of very large proportions of calcium carbonate (≥ 20% w/w in the dry powder ingredients) opens new possibilities which have not yet been explored [4, 26, 32-33].

Several varieties of calcium carbonate (in increasing order of solubility of the $CaCO_3$ phase: calcite (C), aragonite (Ar), vaterite (V) and amorphous calcium carbonate (ACC)) can be encountered in nature [34]. Calcium carbonates of biological origin (nacre and coral) and their derivatives have been used as biocompatible and bioactive bone substitutes in the form of powder, porous ceramic or associated with organic gels for more than 20 years [35-39].

Very recently, Combes et *al.* demonstrated the feasibility of calcium carbonate-based biomedical cements consisting of 100% $CaCO_3$ [40-42]. In order to propose a wide range of cement compositions, we present here a $CaCO_3$-CaP mixed cement concept which is based on the idea that biphasic cements could be prepared which could behave in the same way as biphasic ceramics. Calcium carbonate and biomimetic apatites appear to be one of the most interesting associations for bone filling and repair as biodegradation could be controlled by the proportion of the more soluble $CaCO_3$ in the final cement composition. The $CaCO_3$-CaP mixed cement concept is based on the reactivity of biphasic or triphasic mixtures of highly reactive calcium carbonate and calcium phosphate powders comprising amorphous and/or metastable crystalline phases in the presence of small amounts of aqueous medium. Such cements can be simply obtained by mixing calcium carbonate and calcium phosphate phases in aqueous media. Moreover, cements, unlike materials obtained by high temperature sintering or natural materials, can be intimately associated with biologically active molecules (specific proteins, antibiotics, etc.) to improve bone reconstruction [43-44].

In this paper we present our preliminary investigations on this new type of bone cement: $CaCO_3$-CaP mixed cements. FTIR spectroscopy and X-ray diffraction were performed to understand the reactions responsible for the setting and hardening of these cements. Setting kinetics and mechanical properties were also investigated. Cytoxicity tests, a prerequisite before *in vivo* evaluation, were also performed.

Materials and Methods

Preparation and characterisation of powders

Calcium carbonate crystalline phases (aragonite (Ar) and vaterite (V)) were prepared by double decomposition between a calcium chloride solution (7.35 g in 500 ml of deionized water for Ar; 36.75 g in 250 ml of deionized water for V) and a sodium carbonate solution (5.30 g + 0.08 g strontium chloride in 500 ml of deionized water for Ar; 26.50 g in 250 ml of deionized water for V) at 100°C for aragonite and at 30°C for vaterite. Then the precipitates were filtered and washed with 1 litre of deionized water.

Crystalline and amorphous calcium phosphate phases were prepared by double decomposition between a calcium nitrate solution (86.74 g in 600 ml of deionized water for dicalcium phosphate dihydrate (DCPD or brushite; $CaHPO_4$. $2H_2O$); 47 g in 500 ml of deionized water + 20 ml of ammonium hydroxide solution at 20 % for amorphous tricalcium phosphate (TCPam; $Ca_3(PO_4)_2$. nH_2O)) and an ammonium dihydrogenphosphate solution (42.26 g in 1400 ml of deionized water + 20 ml of ammonium hydroxide solution at 20 %) for DCPD synthesis and a di-ammonium hydrogenphosphate solution (26 g in 1300 ml of deionized water + 20 ml of ammonium hydroxide solution at 20 %) for TCPam. Then the precipitates were rapidly filtered and washed (with 2 litres of deionized water for DCPD and 7 litres of deionized water + 35 ml of ammonium hydroxide solution at 20 % for TCPam). Heat treatment of the amorphous tricalcium phosphate at 400°C during 30 minutes was then carried out to eliminate water associated with crystals while keeping amorphous structure.

After filtration and washing, the precipitates were lyophilised and the powders stored in a freezer.

All the synthesised powders were characterised by transmission FTIR spectroscopy from KBr pellets (Perkin Elmer FTIR 1600 spectrometer) and X-ray diffraction (Inel CPS 120 diffractometer) using a Co anticathode.

Preparation and characterisation of the cements

The cement powders were made up of a mixture of metastable calcium carbonate and calcium phosphate phases; $CaCO_3$ made up at least 40 % (w/w) of the cement dry powder ingredients. The cement paste was obtained by mixing the powders, which had been first homogenised in a mortar, with an appropriate amount of liquid phase (either deionized water or sodium chloride solution (0.9 % w/w)). The amount of solution was determined to allow the formation of a mouldable paste. We chose to test the use of isotonic solution (0.9 % (w/w)

NaCl solution) as it is already the liquid phase of some cements (like alpha-BSM®) and because it could open the possibility to use blood serum as liquid phase.
The wet paste was placed in a sealed container saturated with H_2O at 37°C for setting and hardening. *In vitro* cement evolution in an atmosphere saturated with water can be compared to *in vivo* cement evolution in contact with biological tissues.

The carbonate content of cements was checked using a CO_2 coulometer (Coulometrics Inc., USA) that measures the CO_2 released during sample dissolution in acidic conditions ($HClO_4$, 2M) and in a closed system. The CO_2 released is transferred into a photometric cell in a non-aqueous medium and titrated through an acid-base reaction [45].
To further characterize the carbonated apatite formed after cement setting and hardening, we decomposed the ν_2CO_3 domain according to the work of Bohic and co-workers [46]. Three bands can be detected by FTIR spectroscopy at 867, 872 and 879 cm^{-1} which have been respectively assigned to type A carbonated apatite (carbonate ions substituted for OH ions in the hydroxyapatite structure), type B carbonated apatite (carbonate ions substituted for phosphate groups in the hydroxyapatite structure) and non-apatitic carbonate ions probably located at the surface of the crystals. In addition, the ν_2CO_3 bands may be superimposed on a broad band due to HPO_4^{2-} ions which might be present in such PCA analogous to bone mineral. This band has been shown to interfere on the low wavenumber side of the ν_2CO_3 domain [47]. However, the broadness of this band does not cause significant interference with the CO_3^{2-} band. The evaluation of carbonate type A/type B and non-apatitic/type B ratios (noted A/B and non-Ap/B ratios, respectively) by FTIR spectroscopy was performed by curve-fitting in the ν_2CO_3 domain (900-800 cm^{-1}) using Grams/32 software (Galactic Industries Corporation). In this domain, the $CaCO_3$ crystal types (calcite, aragonite, vaterite) showed a sharp and intense absorption band at 855 cm^{-1} for aragonite and 875 cm^{-1} for vaterite and calcite.
Observation of cements by scanning electron microscopy (SEM) was carried out using a Leo 435 VP microscope. Small pieces of hardened and dried cement samples were placed and fixed on a support with double faced carbon tape.

Setting time and compressive strength measurements

The setting rate of the cement was followed with a TA–XT2 Texture Analyser fitted with a cylindrical needle (0.7 mm in diameter). The setting time was considered to be reached when the paste developed a resistance to needle penetration greater than 600 g/mm^2.

The compressive strength of the cement was evaluated using a Hounsfield Series S apparatus. The cement paste was placed in a cylindrical mould (height / diameter ratio ≅ 2 and diameter equal to 10.5 mm) and packed tightly in order to eliminate air bubbles trapped in the paste. The paste was left to set and harden at 37°C in a sealed container saturated with water for 1 day. The hardened cement was withdrawn from the container and left to dry for 1 week at 37°C. The cement was then removed from the mould and the compressive test performed.

Indirect cytotoxicity evaluation

The indirect cytotoxicity was assessed by an extraction method according to NFEN30993-5 ISO 10993-5 [48-49]. Osteoprogenitor cells arising from human bone marrow according to Vilamitjana-Amédée et *al.* with some modifications [50] were used for testing the extracts and cultured in Iscove Modified Dulbecco's Medium (IMDM, Sigma Aldrich, France) containing 10% foetal calf serum (FSC, Sigma, France).

The cells were seeded at a density of 40 000 cells/cm^2 in 96-well microtiter plates (Nunc, Denmark) and the culture was maintained at 37°C for 96 h after cell plating. At subconfluency the medium was replaced by the cement extraction vehicle. To obtain extraction vehicles, fragments of sterile hardened cement were immersed in IMDM. The ratio of the sample surface area to the volume of the vehicle was 5 cm^2/ml. Extractions were performed in borosilicate glass tubes at 37°C for 120 h without stirring according to the standard procedures. Borosilicate tubes containing identical extraction vehicles with either no cement or a solution of phenol at a concentration of 6.4 g/l (known to be cytotoxic) were processed under the same conditions to provide negative and positive controls, respectively. The medium was removed and replaced by control extracts at various concentrations (100% (v/v), 50% (v/v), 10% (v/v), 1% (v/v)) in the culture medium for 24 h at 37°C. At the end of the extract incubation period, tests were performed: cell viability (Neutral Red assay) and cell metabolic activity (MTT assay) [51-52]. The intensity of the colors obtained (red and blue respectively) is directly proportional to the viability and metabolic activity of the cell population and inversely proportional to the toxicity of the material. Indirect cytotoxicity tests were duplicated for each cement composition. The mean values of absorbance measurements obtained from colorimetric tests and their corresponding standard deviation (± SD) were

calculated. The results were expressed as a percentage of the negative control (plastic) tested during the same experiment.

Results

Three examples of initial powder mixtures that lead to hardened cements are reported in table 1. The liquid-to-solid ratio (L/S) ranges between 0.5 and 0.72 depending on the composition of the powder mixture. For a given powder mixture composition, this ratio can vary to some extent but the value reported corresponds to the optimum final mechanical resistance of the cement.

The setting time and the compressive strength of (Ar+V+Br), (V+Br) and (V+TCPam) cements are reported in table 1. Just after mixing the powders with the liquid phase, the paste was viscous and easily mouldable for several minutes. The cements set within one hour and hardened. Slower setting (i.e. longer setting times) and higher compressive resistance were measured for cements prepared with vaterite and brushite mixtures. In all cases**,** the compressive strength remained rather weak (≤ 13 MPa).

Figure 1 shows the X-ray diffraction (XRD) diagrams of two examples of $CaCO_3$-CaP mixed cements after setting and hardening. The final composition of such cements comprises a poorly crystalline apatite analogous to bone mineral which can be associated with a calcium carbonate crystalline phase (vaterite, aragonite or calcite) depending on the relative amount of phosphate compound in the initial mixture. For example, vaterite was present in the final composition of (V+Br) cement (see figure 1) and also of (V+TCPam) cement. The XRD diagram of the (V+TCPam) cement (not presented) was similar to that of (V+Br) cement. A small amount of brushite was seen to remain in the hardened (V+Br) cement. For (Ar+V+Br) cement, no crystalline $CaCO_3$ phase was detected by X-ray diffraction analysis and the corresponding X-ray diagram is quite analogous to that of bone (see figure 1).

The FTIR spectra of different mixed $CaCO_3$-CaP cements analyzed after setting and hardening at 37°C are presented in figure 2. The analogy of (Ar+V+Br) cement with bone mineral is confirmed by FTIR spectroscopy. However, we can clearly notice the higher intensity of the absorption bands in the ν_2CO_3 and ν_3CO_3 domains revealing the presence of a highly carbonated apatite and/or calcium carbonate compounds. The decomposition of the ν_2CO_3 domain of (Ar+V+Br) cement spectrum into 6 subbands (see figure 3) revealed the formation of an AB type carbonated apatite analogous to bone mineral. The calculated area ratios based on FTIR data were 0.40 and 0.88 for A/B and non-Ap/B ratios respectively. These different values indicate that B type carbonate is the main species and that a large

proportion of CO_3^{2-} (non-apatitic CO_3^{2-}) is located at the surface of apatite crystals. The broad band, assigned to HPO_4^{2-} ions, appeared clearly on the low wavenumber side of the ν_2CO_3 domain.

In addition, the decomposition of the ν_2CO_3 domain of (Ar+V+Br) cement reveals a peak at 855 cm^{-1} assigned to carbonate groups in aragonite. The presence of a small amount of aragonite associated with PCA was confirmed by the presence of the two characteristic absorption bands of aragonite at 700 and 713 cm^{-1} in the ν_4CO_3 domain (figure 2). These results showed that the detection limit of FTIR spectroscopy for aragonite is higher than that of X-ray diffraction.

For (V+Br) cement, the characteristic bands of vaterite at 875 cm^{-1} and 745 cm^{-1} can be distinguished in the ν_2CO_3 and ν_4CO_3 domains respectively which confirmed the presence of untransformed vaterite in the hardened cement also detected by X-ray diffraction analysis.

For the two kinds of cement, we observed a decrease of the FTIR band width of all CO_3 and PO_4 vibration bands compared to those of bone mineral suggesting a better crystallinity of PCA in cement than in bone. The X-ray diffraction peaks for bone also appeared broader than those of the cements (see figure 1).

The total carbonate content in the initial powder mixture and the hardened cement for three examples of $CaCO_3$-CaP mixed cements are reported in table 2. It varies from 10 % to 21 % for (Ar+V+Br) cement and (V+TCPam) cement respectively. In all cases, the strong decrease of CO_3^{2-} content for hardened cements compared to powder mixtures indicates that there is release of CO_2 during the setting reaction. The formation of a highly carbonated apatite analogous to bone mineral was confirmed for (Ar+V+Br) cement; the weight proportion of CO_3^{2-} was 10 %. This value is in the range of carbonate contents found for human bone.

Figure 4 shows SEM micrographs of (V+TCPam) and (V+Br) cement. The hardened cements appeared to be mainly formed of a poorly crystalline phase. For (V+Br) cement, the platelet crystals of brushite disappeared after setting and hardening.

Many spherical micropores can be seen in (V+TCPam) cement (see figures 4c and 4d). These micropores do not however seem to be interconnected.

The results of the indirect biocompatibility study following incubation of cells with cement extracts at different dilutions, presented in figure 5, showed no cytotoxicity effect of cements prepared with (Ar+V+Br) and (V+Br) mixtures. Values of cell viability obtained for undiluted extracts were (102 ± 10) % for (Ar+V+Br) and (114 ± 14) % for (V+Br) which are close to the 100% value for the referenced control (plastic). The results of metabolic activity

measurement for undiluted extract were also close to the 100 % value for the referenced control (plastic) ((94 ± 6) % for (Ar+V+Br) and (100 ± 13) % for (V+Br)). No significant difference was ever noted for the two cement compositions or between the different extract dilutions (1 to 100 %).

Discussion

$CaCO_3$-CaP mixed cement compositions

The calcium carbonate-calcium phosphate ($CaCO_3$-CaP) mixed cements presented in this paper and the trial compositions, especially (V+Br; 1:1) and (V+TCPam; 1:1), are the first $CaCO_3$-CaP mixed cements for biomedical applications with more than 20 % calcium carbonate(s) in the initial powder mixtures. Several CaP biomedical cement formulations that incorporate a certain proportion of $CaCO_3$ have been designed to improve the mechanical properties of the cement or its compliance or to create macroporosity but the proportion of calcium carbonate in such cement compositions did not exceed 15% (w/w) and the final product did not contain a calcium carbonate phase [4, 26, 32-33]. However, we can note that very recently Combes and co-workers demonstrated the feasibility of calcium carbonate biomedical cements composed of 100 % $CaCO_3$ [41].

The $CaCO_3$-CaP mixed cement compositions proposed here can be prepared straightforwardly by simply mixing water (liquid phase) with calcium carbonate phase(s) and a calcium phosphate phase (solid phase) which can be easily obtained by precipitation. The initial composition of $CaCO_3$-CaP mixed cements comprised a powder biphasic or ternary mixture including metastable calcium carbonate crystalline phase(s) (≥ 40 % w/w in the dry powder ingredients) and a crystalline or amorphous calcium phosphate phase.

Among all the powder combinations tested, three dry powder compositions including at least 42 % of calcium carbonate phase(s) appeared as promising formulations for $CaCO_3$-CaP mixed cements. However, the initial cement compositions are not limited to the three presented in table 1 and other ($CaCO_3$+CaP) powder mixtures ((Ar+Br; 1:2; L/S = 0.5) and (V+Ar+TCPam; 1:1:3; L/S = 0.8) mixtures for example) were in fact tested but led to a setting paste with poor compressive strength. However, not all the parameters of these complex mixtures have been optimised and mechanical resistance could certainly be improved with further investigations on these cement compositions.

In a preliminary study of $CaCO_3$-CaP mixed cement compositions, especially initial mixtures of aragonite and brushite (1:2 (w:w)) for example), FTIR and XRD analyses revealed that the

resulting cement was made up of brushite, aragonite and a small quantity of poorly crystalline apatite, the formation of which appeared to determine cement setting. This was an original and interesting final composition that can be compared to the brushite-type calcium phosphate cement setting reaction which produces DCPD [3]. The final composition of (Ar+Br) cement associating mostly DCPD and aragonite which have a higher solubility than PCA, probably infers a high biodegradation rate along with less acid release than for brushite calcium phosphate cements. Indeed, aragonite (basic component) would partly moderate the drop of pH accompanying the transformation of DCPD into PCA. However, as the setting and hardening time of (Ar+Br) cement can be longer than 12 h, we decided to discard this composition from future investigations.

FTIR spectroscopy and X-ray diffraction analyses showed that for the cement compositions presented herein a poorly crystalline apatite (PCA) analogous to bone mineral (AB type carbonated apatite) associated or not with untransformed crystalline CaP and/or $CaCO_3$ phases is involved in the final cement compositions. In addition, the preparation of $CaCO_3$-CaP mixed cements either with water or NaCl solution (0.9 % w/w) did not significantly modify the composition, the setting or hardening reactions.

AB type carbonated apatites analogous to bone mineral can be described by the following general chemical formula [16]:

$$Ca_{10-x}(PO_4)_{6-x}(HPO_4 \text{ and } CO_3)_x(OH \text{ and } ½\ CO_3)_{2-x}$$

For (Ar+V+Br) cement, the high value of the non-Ap/B ratio determined from FTIR data indicated that a large proportion of carbonate ions in the PCA were in the hydrated layer (non-apatitic CO_3^{2-} ions) [16, 18]. This observation is interesting as carbonate species slow down the maturation of apatite nanocrystals and stabilise them in their native very reactive form.

In addition, the presence of non-apatitic HPO_4^{2-} and PO_4^{3-} groups, located in the hydrated PCA surface layer, can be revealed by decomposition of the ν_4 PO_4 band of the cement FTIR spectrum [16, 18].

An interesting ability of these $CaCO_3$-CaP mixed cement compositions is to reach very high carbonate contents and even to produce in most cases biphasic systems ($CaCO_3$ and CaP compounds) offering a wide range of $CaCO_3$-CaP mixed final compositions. Indeed, by comparing (V+Ar+Br) and (V+Br) cement final composition (see figure 1), we can clearly see that the proportion of calcium carbonate associated with PCA varied significantly and we can consider preparing and adapting the cement composition and thus its biodegradation

properties depending on the biomedical applications. However, from these preliminary investigations it appears difficult to precisely anticipate the final cement composition due to the CO_2 release that occurs during the setting and hardening reactions (see equation 1 hereafter). The composition of the apatite formed cannot be precisely determined due to the presence of $CaCO_3$ phase(s) remaining in the hardened cement and to the lack of analytical methods to evaluate the proportion of $CaCO_3$ in these biphasic cements. Part of our future investigations into such cement compositions will focus on setting-up a quantitative method based on FTIR spectroscopy and/or X-ray diffraction analysis to characterize the hardened cement composition and thus indirectly quantify the CO_2 released during cement preparation.

The possibility of having a large amount of calcium carbonate associated with PCA in the hardened cement is an interesting feature. Indeed, due to the higher solubility of calcium carbonate compared to apatite, we can expect a faster biodegradation rate for $CaCO_3$-CaP mixed cements than for CaP cements. The association of $CaCO_3$ and PCA in the cement final composition can be compared to the well-developed biphasic calcium phosphate ceramics associating CaP phases with different solubilities (hydroxyapatite and tricalcium phosphate for example) for a better control of bioceramic biodegradation and bone reconstruction processes [21].

As the $CaCO_3$-CaP mixed cement concept presented in this paper involved the formation of an apatitic phase analogous to bone mineral after setting, we can consider such compositions as biomimetic like most of the well-known and studied CaP cements [14].

Setting and hardening reaction

In the case of $CaCO_3$-CaP mixed bone cements, the type of reaction responsible for setting and hardening differs from that of CaP-based cements in several aspects. CaP biomedical cements can be classified into two main categories: apatite and brushite cements that respectively lead to hydroxyapatite and brushite (dicalcium phosphate dihydrate: DCPD) which could be converted into apatite *in vivo* [1, 53-54]. Two main types of setting reactions can be distinguished for CaP cements: acid-base reaction and/or phase transformation (fast hydrolysis for example) of a metastable CaP phase into apatite associated with respectively more or less pH variation of the paste during setting. The involvement of acid-base and/or phase transformation reactions in $CaCO_3$-CaP mixed bone cements will be discussed hereafter.

We have shown that the total content of CO_3^{2-} in the hardened cement was, in all cases, lower than the initial CO_3^{2-} level in the powder mixture.

In the case of the $CaCO_3$-brushite mixed cements presented herein ((V+Br) and (Ar+V+Br) cements for example), the setting reaction appeared to be essentially related to the formation of a highly carbonated nanocrystalline apatite analogous to bone mineral by reaction of DCPD onto part or almost all of the $CaCO_3$ metastable crystalline phase(s). Indeed, for all cement compositions tested, no setting occurs if PCA is not formed. The decrease of the CO_3^{2-} level is related to the reaction of brushite hydrogenophosphate ions on carbonate ions of vaterite or aragonite according to the following chemical reaction:

$$2\ HPO_4^{2-} + CO_3^{2-} \rightarrow 2\ PO_4^{3-} + CO_2 + H_2O \qquad \text{Eq. (1)}$$

As vaterite is a slightly basic component and brushite an acidic one, this setting reaction can be related to a rather slow acid-base setting reaction of CaP cements. The release of CO_2 induces microporosity (see figure 4) in the hard cement without visible swelling. In addition, the water molecules from the DCPD transformation and the above reaction fill up the pores between crystals and participate in the formation of a hydrated layer on the PCA nanocrystals. SEM observations (figures 4a and 4b) support the fact that DCPD was transformed into PCA by a dissolution-reprecipitation process as platelet crystals of DCPD are no longer visible in the hardened cement and the remaining phase appeared poorly crystallized. However, a few lentil-like crystals of vaterite can be distinguished on the surface (see figure 4b).

In the case of (V+TCPam) cement, upon contact with an aqueous solution, fast hydrolysis of the amorphous tricalcium phosphate into a poorly crystalline apatite phase is involved in the cement setting reaction. A reaction between phosphate and carbonate ions (equation 1) can also occur and participate in the formation of a poorly crystalline carbonated apatite. This cement composition can be related to the α-BSM® cement concept (ETEX Corp.) for which the setting reaction also involves the fast hydrolysis of the amorphous CaP phase into apatite [53]. The crystalline metastable CaP phase (DCPD) in the α-BSM® cement composition acts as a template to facilitate apatite crystal nucleation and growth. By analogy with α-BSM®cement, which is made up of a mixture of DCPD and TCPam, a preliminary study on (V+TCPam) cement showed that the presence of metastable crystalline phases such as vaterite appears essential for cement setting and hardening since upon admixture with water, pure TCPam powder alone did not harden whereas the paste formed by a mixture of TCPam and vaterite set and hardened. However, we have shown that a large amount of untransformed

vaterite can be detected by FTIR spectroscopy and X-ray diffraction techniques in the hardened cement suggesting that, in $CaCO_3$-CaP mixed cements, the initial vaterite crystals serve as a template for the crystallization of a more stable calcium phosphate phase. Furthermore, the stabilisation of vaterite and other calcium carbonate crystalline phases in the presence of phosphate ions has been reported by several authors [55-56]. Thus, the dissolution-reprecipitation process of vaterite can be (partly) inhibited due to the adsorption of phosphate ions onto the $CaCO_3$ crystal surface.

In the case of (V+TCPam) cement, the formation of OH^- and HPO_4^{2-} ions during the formation of the poorly crystalline apatite from TCPam hydrolysis can be related to the hydrolysis of PO_4^{3-} ions according to equation 2 [57]:

$$PO_4^{3-} + H_2O \rightarrow OH^- + HPO_4^{2-} \qquad \text{Eq. (2)}$$

This chemical reaction is endothermic which could explain the necessity to warm the paste, to 37°C for example, for faster setting.

For the (V+TCPam) cement, the slight acidification of the paste during the hydrolysis of TCPam along with the presence of carbonate ions from the calcium carbonate source could explain the release of part of the carbonate. In addition, a fraction of carbonate ions can also be incorporated in the apatite lattice.

We can assume that the reactions involved during $CaCO_3$-CaP mixed cement formation do not cause a significant pH variation of the paste due to the presence of large amounts of $CaCO_3$ (basic component) that can moderate the pH drop during PCA formation. Moreover, no visible change in pH (solution color) was observed when fragments of hardened cement were immersed and equilibrated in the IMDM solution used for the indirect cytotoxicity test which means that the products of the setting reaction and/or the residues are, as expected, not highly acidic and/or basic compounds. In addition, no significant rise in paste temperature was detected during paste preparation, setting or hardening.

Even if the result of the setting reaction might be different *in vivo* and *in vitro* especially due to the reactivity of the phases in the hardened cement, one of the remaining questions concerned the future of these constituting phases once implanted *in vivo*. The evolution of DCPD and PCA *in vivo* is quite well documented as these CaP phases are involved in the well-developed CaP bioceramics and cements whereas no precise data have been reported for the *in vivo* physical-chemical evolution of metastable calcium carbonate phase(s) such as

vaterite or aragonite. Unlike for calcium phosphates, only a few studies reported the level of saturation of biological fluids with respect to calcium carbonate crystalline phase [58-59]. However, the work of Maeda *et al.* showed the high apatite-forming ability of titania-vaterite composite in simulated body fluid solution due to the high solubility of vaterite suggesting that vaterite is unstable in biological fluids [60]. Thus, we can consider that metastable $CaCO_3$ (vaterite) in hardened cement will dissolve or be transformed rather rapidly after implantation.

Properties of $CaCO_3$-CaP mixed cements

Even though the compressive strength of the $CaCO_3$-CaP mixed cement remained poor in all cases (≤ 13 MPa), this would not be determinant for *in vivo* applications such as bone filling especially in low mechanical stress locations. Moreover these properties can probably be improved by optimising the specific surface area of the reactive powders and thus the L/S ratio.

The excellent cytocompatibility of the $CaCO_3$-CaP mixed cement compositions revealed by indirect cytotoxicity evaluation is probably related to the stability of pH involved in the setting reaction and the low solubility of the $CaCO_3$ and CaP in the final composition. Another advantage of such $CaCO_3$-CaP mixed cements is that their *in vivo* biodegradation would release calcium, carbonate and phosphate ions and/or CO_2 which are non-cytotoxic metabolites as they are under the control of the organism.

A recent study on fresh anatomical pieces, showed that we can consider preparing $CaCO_3$-CaP mixed cements with the patient's blood as liquid phase [40]. In addition, we can take advantage of the control of pH, temperature and final cement composition (resorption properties) of $CaCO_3$-CaP mixed cement by associating the paste with biologically active components (growth factors, specific proteins, platelets) promoting tissue repair, which could be progressively released after implantation.

Conclusions

Several original $CaCO_3$-CaP mixed cement compositions containing at least 40 % calcium carbonate (w/w in the dry powder ingredients) have been proposed. The setting and hardening reaction is essentially related to the formation of a poorly crystalline carbonated apatite and the composition of the hardened cement can be biphasic (metastable crystalline $CaCO_3$ phase and poorly crystalline apatite). The possibility to control and adapt the composition of the

final phase(s) and consequently the cement biodegradation properties is an interesting feature of these cements.

We did not detect any toxic effects on human osteoprogenitor cells suggesting good cytocompatibility of the $CaCO_3$–CaP mixed cement compositions.

References

1. Bohner M. Calcium orthophosphates in medicine: from ceramics to calcium phosphate cements. Injury, Int.J. Care Injured 2000; 31: S-D37-47.

2. Brown WE, Chow LC. A new calcium phosphate, water-setting cement. In PW Brown editor, Cements Research Progress 1986,Westerville OH, The Am. Ceram. Soc. (1987), 352-379.

3. Mirtchi AA, Lemaître J, Terao N. Calcium phosphate cements: study of the β-tricalcium phosphate-monocalcium phosphate system. Biomaterials 1989; 10: 475-480.

4. Constantz BR, Ison IC, Fulmer MT, Poser RD, Smith ST, VanWagoner M, Ross J, Goldstein SA, Jupiter JB, Rosenthal DI. Skeletal repair by in situ formation of the mineral phase of bone. Science 1995; 267: 1796-1798.

5. Lee D, Rey C, Aiolova M. Methods and products related to the physical conversion of reactive amorphous calcium phosphate, US patent (1996) 08/729, 344.

6. Ginebra MP, Fernandez E, De Maeyer EA, Verbeeck RM, Boltong MG, Ginebra J, Driessens FC, Planell JA. Setting reaction and hardening of apatitic calcium phosphate cement. J Dent Res 1997; 76: 905-912.

7. Kon M, Miyamoto Y, Asaoka K, Ishikawa K, Lee HH. Development of calcium phosphate cement for rapid crystallization to apatite. Dent Mater J 1998; 17: 223-232.

8. Hatim Z, Frèche M, Keribech A, Lacout JL. The setting mechanism of a phosphocalcium biological cement. Ann Chim Sci Mat 1998; 23: 65-68.

9. Dos Santos LA, De Oliveira LC, Rigo EC, Carrodeguas RG, Boschi AO, De Arruda AC. Influence of polymeric additives on the mechanical properties of α-tricalcium phosphate cement. Bone 1999; 25: 99S-102S.

10. De Maeyer EA, Verbeeck RM, Vercruysse CW. Conversion of octacalcium phosphate in calcium phosphate cements. J Biomed Mater Res 2000; 52: 95-106.

11. Braye F, Irigaray JL, Jallot E, Oudadesse H, Weber G, Deschamps N, Deschamps C, Frayssinet P, Tourenne P, Tixier H, Terver S, Lefaivre J, Amirabadi A. Resorption kinetics of osseous substitute: natural coral and synthetic hydroxyapatite. Biomaterials 1996; 17: 1345-1350.

12. Jamali A, Hilpert A, Debes J, Afshar P, Rahban S, Holmes R. Hydroxyapatite/calcium carbonate (HA/CC) vs. plaster of Paris: A histomorphometric and radiographic study in a rabbit tibial defect model. Calcif Tissue Int 2002; 71: 172-178.

13. Ikenaga M, Hardouin P, Lemaître J, Andrianjatovo H, Flautre B. Biomechanical characterization of a biodegradable calcium phosphate hydraulic cement: A comparison with porous biphasic calcium phosphate ceramics. J Biomed Mater Res 1998; 40: 139-144.

14. Rey C, Tofighi A, Mounic S, Combes C, Lee D. Biomimetism and Calcium Phosphate Cements. In Mainard D, Louis JP, editors. Actualités en Biomatériaux vol. VI, Paris: Editions Romillat, 2002. p. 27-37

15. Rey C, Lian J, Grynpas M, Shapiro F, Zylberberg L, Glimcher MJ. Non-apatitic environments in bone mineral: FT-IR detection, biological properties and changes in several disease states. Connect Tissue Int 1989; 21: 267-273.

16. Cazalbou S, Combes C, Eichert D, Rey C. Adaptative physico-chemistry of bio-related calcium phosphates. J Mater Chem 2004; 14: 2148-2153.

17. Rey C, Strawich E, Glimcher MJ. Non-apatitic environments in Ca-P biominerals; implications in reactivity of the mineral phase and its interactions with organic matrix constituents. In: Allemand D, Cuif JP, editors. Biomineralizations. Bulletin Océanographique de Monaco, Monaco, 1994; 14,1: 55-64

18. Rey C, Hina A, Tofighi A, Glimcher MJ. Maturation of poorly crystalline apatites: chemical and structural aspects in vivo and in vitro. Cells Mater 1995; 5: 345-356.

19. Elliott JC. Structure and Chemistry of the Apatites and Other Calcium Orthophosphates. In: Studies in Inorganic Chemistry, vol. 18, Elsevier Amsterdam , 1994. p. 191-304.

20. Legeros RZ. Biodegradation and bioresorption of calcium phosphate ceramics. Clin Mater 1993; 14: 65-88.

21. Daculsi G, Laboux O, Malard O, Weiss P. Current state of the art of biphasic calcium phosphate bioceramics. J Mater Sc: Mater Med 2003; 14: 195-200.

22. Chiroff RT, White EW, Weber JN, Roy DM. Tissue ingrowth of Replamineform implants. J Biomed Mater Res 1975; 9: 29-45.

23. Damien E, Revell PA. Coralline hydroxyapatite bone graft substitute: a review of experimental studies and biomedical applications. J Applied Biomaterials and Biomechanics 2004; 2: 65-73.

24. Walsh WR, Chapman-Sheath PJ, Cain S, Debes J, Bruce WJM, Svehla MJ, Gillies RM. A resorbable porous ceramic composite bone graft substitute in a rabbit metaphyseal defect model. J Othop Res 2003; 21: 655-661.

25. Rawlings CE, Wilkins RH, Hanker JS, Georgiade NG, Harrelson JM. Evaluation in cats of a new material for cranioplasty: a composite of plaster of Paris and hydroxylapatite. J Neurosurg 1988; 69: 269-275.

26. Mirtchi AA, Lemaître J, Munting E. Calcium phosphate cements: study of the β-tricalcium phosphate-dicalcium phosphate-calcite cements. Biomaterials 1990; 11: 83-88.

27. Ohura K, Bohner M, Hardouin P, Lemaître J, Pasquier G, Flautre B. Resorption of, and bone formation from, new β-tricalcium phosphate-monocalcium phosphate cements: An in vivo study. J Biomed Mater Res 1996; 30: 193-200.

28. Nillson M, Fernandez E, Sarda S, Lidgren L, Planell JA, Characterization of a novel calcium phosphate/sulphate bone cement. J Biomed Mater Res 2002; 61: 600-607.

29. Bohner M. New hydraulic cements based on α-tricalcium phosphate-calcium sulfate dihydrate mixtures. Biomaterials 2004; 25: 741-749.

30. Brecevic L, Nielsen AE. Solubility of amorphous calcium carbonate. J Crystal Growth 1989; 98: 504-510.

31. Heughebaert JC, Nancollas GH. Kinetics of crystallization of octacalcium phosphate. J Phys Chem 1984 ; 88 : 2478-2480.

32. Khairoun I, Boltong MG, Driessens FCM, Planell JA. Effect of calcium carbonate on the compliance of an apatitic calcium phosphate bone cement. Biomaterials 1997; 18: 1535-1539.

33. Fernandez E, Gil FJ, Best SM, Ginebra MP, Driessens FCM, Planell JA. Improvement of the mechanical properties of new calcium phosphate bone cements in the $CaHPO_4$-α-$Ca_3(PO_4)_2$ system: Compressive strength and microstructural development. J Biomed Mater Res 1998; 41: 560-567.

34. Meldrum FC. Calcium carbonate in biomineralisation and biomimetic chemistry. Int Mater Rev 2003; 48: 187-224.

35. Atlan G, Delattre O, Berland S, LeFaou A, Nabias G, Cot D, Lopez E. Interface between bone and nacre implants in sheep. Biomaterials 1999; 20: 1017-1022.

36. Piattelli A, Podda G, Scarano A. Clinical and histological results in alveolar ridge enlargement using coralline calcium carbonate. Biomaterials 1997; 18: 623-627.

37. Guillemin G, Patat JL, Meunier A. Natural corals used as bone graft substitutes. Bulletin de l'Institut Océanographique de Monaco 1995; 14(3) :67-77.

38. Arnaud E, de Pollak C, Meunier A, Sedel L, Damien C, Petite H. Osteogenesis with coral is increased by BMP and BMC in a rat cranioplasty. Biomaterials 1999; 20: 1909-1918.

39. Souyris F, Pellequer C, Payrot C, Servera C. Coral, a new biomedical material. Experimental and first clinical investigations on Madreporaria. J Maxillofac Surg 1985 ; 13 : 64-69.

40. Fontaine ML, Combes C, Sillam T, Dechambre G, Rey C. New calcium-carbonate-based cements for bone reconstruction. Key Engineering Materials 2005 ; 284-286 : 105-108.

41. Combes C, Miao B, Bareille R , Rey C. Preparation, physical-chemical characterisation and cytocompatibility evaluation of calcium carbonate cements. Biomaterials (accepted).

42. Fontaine ML, Combes C, Mounic S, Rey C. Composition de ciment hydraulique à base de carbonates de calcium. Patent No FR2830249, 2001.

43. Blom EJ, Klein-Nulend J, Wolke JGC, Van Waas MAJ, Driessens FCM, Burger EH. Transforming growth factor-β1 incorporation in a calcium phosphate bone cement: Material properties and release characteristics. J Biomed Mater Res 2002; 59: 265-272.

44. Lucas A, Gaude J, Carel C, Michel JF, Cathelineau G. A synthetic aragonite-based ceramic as bone graft substitute and substrate for antibiotics. Int J Inorg Mater 2001; 3: 87-94.

45. Huffman EWD. Performance of a new automatic carbon dioxide coulometer. Microchemical J 1977; 22: 567-573.

46. Bohic S, Rey C, Legrand A, Sfihi H, Rohanizadeh R, Martel C, Barbier A, Daculsi G. Characterization of the trabecular rat bone mineral: effect of ovariectomy and bisphosphonate treatment. Bone 2000; 26: 341-348.

47. Collins B, Goehl T, Dickson R, Glimcher MJ. The carbonate environment in bone mineral: a resolution-enhanced Fourier transform infrared spectroscopy study. Calcif Tissue Int 1989; 45: 157-164.

48. AFNOR6NF EN 30993-5. Evaluation biologique des dispositifs médicaux. Partie 5: essais concernant la cytotoxicité : Méthodes in vitro. Novembre 1994.

49. ISO10993-5. Biological evaluation of medical devices. Test for cytotoxicity: in vitro methods. 1992

50. Vilamitjana-Amédée J, Bareille R, Rouais F, Caplan AI, Harmand MF. Human bone marrow stromal cells express an osteoblastic phenotype in culture. In Vitro Cell Dev Biol Anim. 1993; 29A: 699-707.

51. Parish CR, Mullbacher A. Automated colorimetric assay for T cell cytotoxicity. J Immunol Methods 1983;58:225-37.

52. Mosmann T. Rapid colorimetric assay for cellular growth and survival: Application to proliferation and cytotoxicity assays. J Immunol Methods 1983;65:55-63.

53. Tofighi A, Mounic S, Chakravarthy P, Rey C, Lee D. Setting reactions involved in injectable cements based on amorphous calcium phosphate. Key Engineering Materials 2001; 192-195: 769-772.

54. Penel G, Leroy N, Van Landuyt P, Flautre B, Hardouin P, Lemaître J, Leroy G. Raman Microspectrometry studies of brushite cement: in vivo evolution in a sheep model. Bone 1999; 25: 81S-84S.

55. Sabbides TG, Koutsoukos PG. The effect of surface treatment with inorganic orthophosphate on the dissolution of calcium carbonate. J Crystal Growth 1996; 165: 268-272.

56. Reddy M, Nancollas GH. Effect of phosphates and phosphonates on nucleation and crystal growth of calcium carbonate. In: Proceedings of the American Chemical Society, division water, air and waste chemistry 1972; 12(2): 212-216

57. Heughebaert JC, Montel G. Conversion of amorphous tricalcium phosphate into apatitic tricalcium phosphate. Calcif Tiss Int 1982; 34: S103-S108

58. Oyane A, Onuma K, Ito A, Kim HM, Kokubo T, Nakamura T. Formation and growth of clusters in conventionnal and new kinds of simulated body fluids. J Biomed Mater Res 2003; 66: 339-348.

59 Larsen MJ, Pearce EIF. Saturation of human saliva with respect to calcium salts. Arch Oral Biol 2003; 48: 317-322.

60. Maeda H, Kasuga T, Nogami M, Apatite formation on titania-vaterite powders in simulated body fluid. J European Ceram Soc 2004; 24: 2125-2130.

Figure 1: X-ray diffraction diagrams of examples of calcium carbonate-calcium phosphate mixed cement compositions after setting and hardening compared to the bone X-ray diffraction diagram. (V: vaterite, Ap: apatite, Br: brushite).

Figure 2: FTIR spectra of examples of calcium carbonate-calcium phosphate mixed cement compositions after setting and hardening compared to the bone FTIR spectrum (V: vaterite, Ar: aragonite).

Figure 3: Decomposition of the ν_2CO_3 band (900-800 cm^{-1}) of (Ar+V+Br) cement FTIR spectrum (4 main subbands: type A (A), type B (B) and non-apatitic (non-Ap) carbonate ions in apatite and carbonate ions (Ar) in aragonite).

Figure 4: SEM micrographs of two types of $CaCO_3$-CaP mixed cements:

a) and b) (V+Br) cement
c) and d) (V+TCPam) cement

Figure 5: Indirect cytotoxicity evaluation of two types of $CaCO_3$-CaP mixed cement compositions ((Ar+V+Br) and (Br+V)):

a) Cell viability
b) Metabolic activity

Table 1: Examples of calcium carbonate-calcium phosphate mixed cement compositions and properties.

Powder mixture	Powder ratio (w:w)	L/S (w/w)	Major final phases	Setting time (min)	Compressive strength (MPa)
(V + Br)	1:1	0.50	PCA+V	60	13.0
(V + TCPam)	1:1	0.72	PCA+V	25	1.8
(Ar + V + Br)	1:2:4	0.71	PCA	30	7.4

L = liquid; S = solid
V = vaterite, Ar = aragonite
Br = Brushite or dicalcium phosphate dihydrate (DCPD)
TCPam: amorphous tricalcium phosphate

Table 2: Carbonate content in $CaCO_3$-CaP mixed cement final compositions.

Powder mixture	**Powder weight ratio**	**Initial powder mixture CO_3^{2-} content (% w/w)[a]**	**Final cement CO_3^{2-} content (% w/w)[b]**
V + Br	1:1 (L/S = 0.5)	30.0 %	17.5 %
V + TCPam	1:1 (L/S = 0.75)	30.0 %	21.2 %
Ar + V + Br	1:2:4 (L/S = 1)	26.7 %	10.0 %

L = liquid; S = solid
V = vaterite, Ar = aragonite
Br = Brushite or dicalcium phosphate dihydrate (DCPD)
TCPam: amorphous tricalcium phosphate
[a] Carbonate content calculated
[b] Carbonate content measured by coulometry

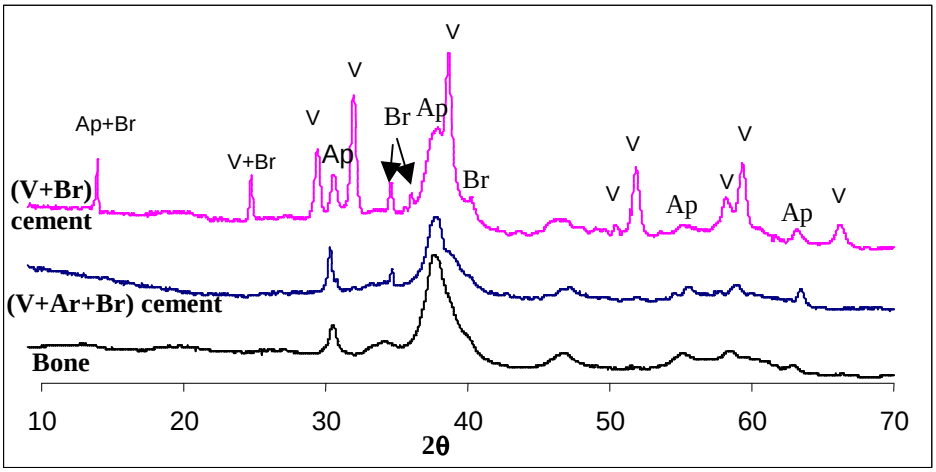
Ap+Br
V+Br
V
V
Ap
Br
Ap
V
Br
V
V
Ap
V
Ap
V
(V+Br) cement
(V+Ar+Br) cement
Bone
10
20
30
40
50
60
70
2θ

Figure 1

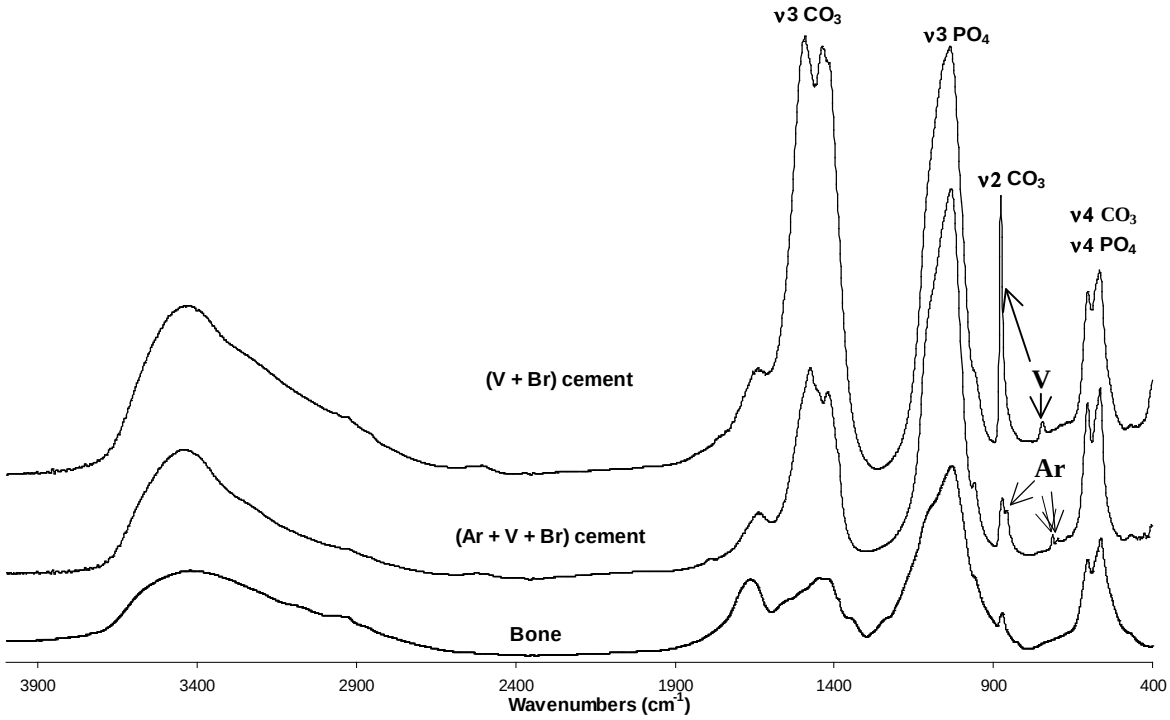
ν3 CO3
ν3 PO4
ν2 CO3
ν4 CO3
ν4 PO4
V
Ar
(V + Br) cement
(Ar + V + Br) cement
Bone
3900
3400
2900
2400
1900
1400
900
400
Wavenumbers (cm-1)

Figure 2

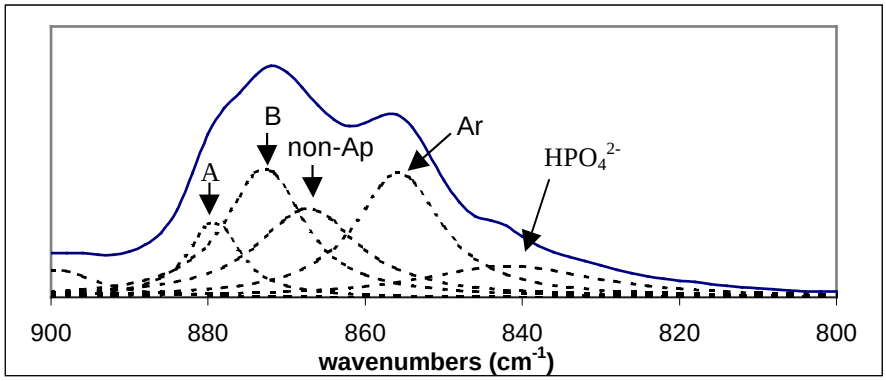

Figure 3

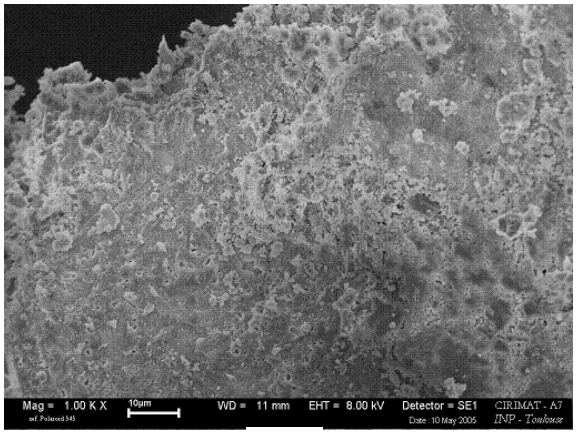

a)

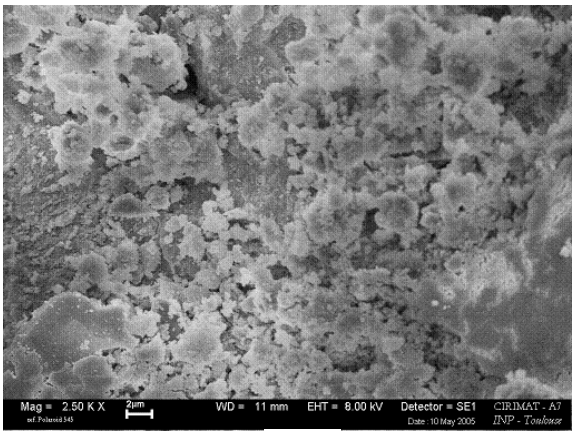

b)

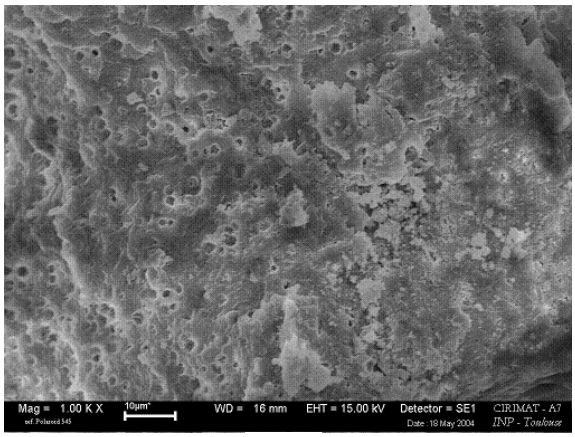

c)

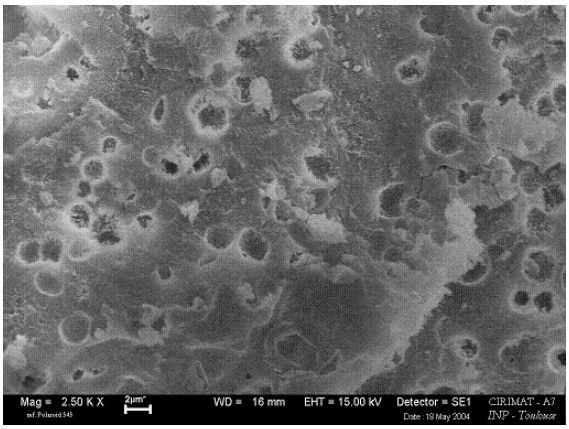

d)

Figure 4

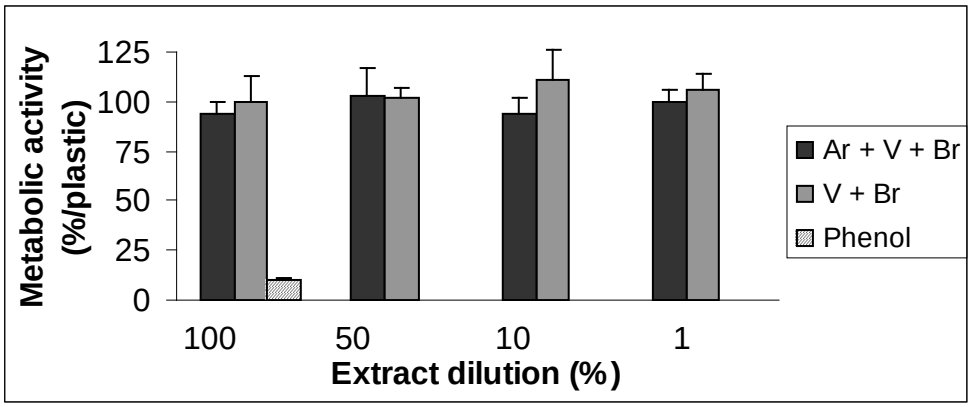
Metabolic activity (%/plastic)
125
100
75
50
25
0
100
50
10
1
Extract dilution (%)
Ar + V + Br
V + Br
Phenol

a)

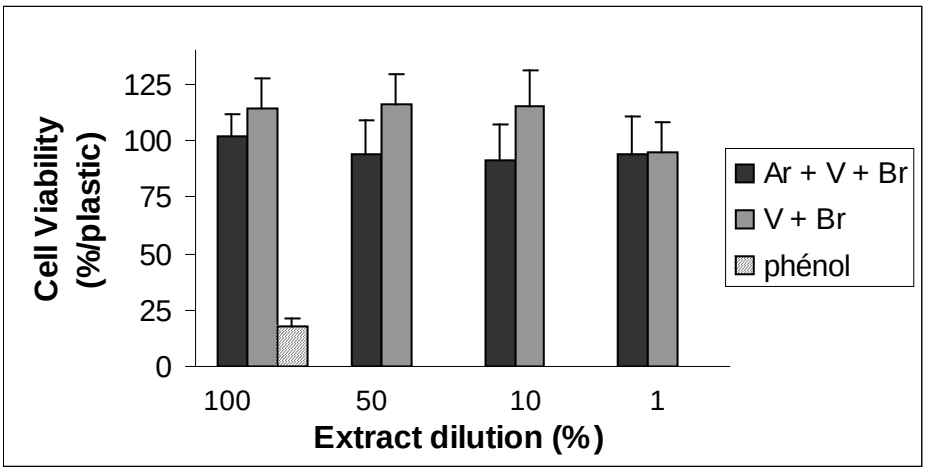
Cell Viability (%/plastic)
125
100
75
50
25
0
100
50
10
1
Extract dilution (%)
Ar + V + Br
V + Br
phénol

b)

Figure 5